Heliyon 10 (2024) e29013

Contents lists available at ScienceDirect

Heliyon

journal homepage: www.cell.com/heliyon

Research article

17β-Estradiol protects female rats from bilateral oophorectomy-induced nonalcoholic fatty liver disease induced by improving linoleic acid metabolism alteration and gut microbiota disturbance

Ying Tian [1], Yuan Xie [1], Xinyu Hong, Zaixin Guo, Qi Yu [*]

Department of Obstetrics and Gynecology, National Clinical Research Center for Obstetric & Gynecologic Diseases, Peking Union Medical College Hospital, Chinese Academy of Medical Sciences & Peking Union Medical College, Peking Union Medical College Hospital (Dongdan campus), No.1 Shuaifuyuan Wangfujing Dongcheng District, Beijing, 100730, China

ARTICLE INFO

Keywords:
Surgical menopause
Nonalcoholic fatty liver disease
Hormone replacement therapy
Linoleic acid

ABSTRACT

After surgical or natural menopause, women face a high risk of nonalcoholic fatty liver disease (NAFLD), which can be diminished by hormone replacement therapy (HRT). The gut microbiota is subject to modulation by various physiological changes and the progression of diseases. This microbial ecosystem coexists symbiotically with the host, playing pivotal roles in immune maturation, microbial defense mechanisms, and metabolic functions essential for nutritional and hormone homeostasis. E_2 supplementation effectively prevented the development of NAFLD after bilateral oophorectomy (OVX) in female rats. The changes in the gut microbiota such as abnormal biosynthetic metabolism of fatty acids caused by OVX were partially restored by E_2 supplementation. The combination of liver transcriptomics and metabolomics analysis revealed that linoleic acid (LA) metabolism, a pivotal pathway in fatty acids metabolism was mainly manipulated during the induction and treatment of NAFLD. Further correlation analysis indicated that the gut microbes were associated with abnormal serum indicators and different LA metabolites. These metabolites are also closely related to serum indicators of NAFLD. An in vitro study verified that LA is an inducer of hepatic steatosis. The changes in transcription in the LA metabolism pathway could be normalized by E_2 treatment. The metabolic perturbations of LA may directly and secondhand impact the development of NAFLD in postmenopausal individuals. This research focused on the sex-specific pathophysiology and treatment of NAFLD, providing more evidence for HRT and calling for the multitiered management of NAFLD.

1. Introduction

The global prevalence of nonalcoholic fatty liver disease (NAFLD) has soared to approximately 38% [1]. NAFLD exhibits great heterogeneity, which is the result of multiple factors, including age, sex, hormonal status, diet, gut microbiota and other metabolic

* Corresponding author.
E-mail addresses: yimuxu1224@163.com (Y. Tian), pumc_xieyuan@163.com (Y. Xie), hongxinyu@pumch.cn (X. Hong), njbg111@126.com (Z. Guo), yuqi2008001@sina.com (Q. Yu).
[1] Contributed equally.

https://doi.org/10.1016/j.heliyon.2024.e29013
Received 20 October 2023; Received in revised form 22 March 2024; Accepted 28 March 2024
Available online 2 April 2024

Abbreviations

17β-estradiol (E_2)
nonalcoholic fatty liver disease (NAFLD)
bilateral oophorectomy (OVX)
hormone replacement therapy (HRT)
hematoxylin and eosin (H&E)
enzyme-linked immunosorbent assay (ELISA)
luteinizing hormone (LH)
follicle-stimulating hormone (FSH)
glutamic oxalacetic transaminase (AST)
glutamic-pyruvic transaminase (ALT)
total cholesterol (TC)
triglyceride (TG)
high-density lipoprotein (HDL)
low-density lipoprotein (LDL)
transmission electron microscopy (TEM)
principal Coordinate Analysis (PCoA)
Gene Ontology (GO)
palmitic acid (PA)
oleic acid (OA)
linoleic acid (LA)
quantitative real-time polymerase chain reaction (qRT-PCR)
methionine- and choline-deficient (MCD)
hepatocellular carcinoma (HCC)
reactive oxygen species (ROS)
metabolic (dysfunction) associated fatty liver disease (MAFLD)

statuses [2]. These factors may exert more complicated interactions. The current leading theory of the pathophysiology of NAFLD is considered to involve “multiple hits” [3], which attempts to fully consider various complex factors that can or cannot be changed.

Women are more protected, at least before natural or surgical menopause, from NAFLD than men. The risk of NAFLD in postmenopausal women appears to be increased and even higher than that of their male counterparts, which could largely be diminished by the use of hormone replacement therapy (HRT) [4]. The corresponding damage and benefits are more obvious in women who undergo bilateral oophorectomy (OVX) before natural menopausal age [4,5], and these women have become one of the targeted populations for interventions to mitigate the morbidity and mortality of NAFLD [6]. The mechanism involved in the protective capacity of estradiol (E_2) against NAFLD is extensive and unclear [7]. For instance, E_2 was able to upregulate miR-125b expression through ERα, protecting against hepatic steatosis in female mice [8], and to downregulate JNK activation and improve mitochondrial function, thus mitigating fatty acid-insulin resistance in hepatocytes [9]. However, deficiency of estrogen signaling was associated with lower levels of PGC1A in the liver, which led to oxidative damage and further exacerbated steatohepatitis in a diet-induced model [10]. Studies focused on the protective potential of E_2 on NAFLD are relatively scarce, so the elucidation of the integrated net mechanism is far from resolved.

The gut microbiota displays dynamic changes at various physiological stages or in the development of different diseases, and it is difficult to define whether these changes are causes or consequences. A certain degree of similarity exists among several metabolic diseases, including NAFLD, obesity and type 2 diabetes [11], while their distinctness is nonnegligible. The term ‘microgenderome’, referring to the sexually dimorphic microbiome, underlines the role it plays in driving sex differences in disease susceptibility [12]. The gut microbiota may intertwine together with sex differences in diseases in obscure ways and potentially become a target for surveillance or treatment. It is difficult to explicitly delineate the relationship among E_2, the microbiota and NAFLD. Preliminary studies have reported that the gut microbiota played a vital role in the progression of estrogen deficiency-induced lipid metabolism disorders by analyzing the gut microbiota and metabolomics of the cecal contents and serum [13]. Moreover, the physiological significance of *gus*-enriched bacteria such as Ruminococcus spp. merits attention, given their direct impact on steroid metabolism in the intestinal milieu, thus potentially modulating the pathophysiology of estrogen-related dysfunctions [14]. More explorations involving more tissue types and bioinformation are needed to reveal these complex mechanisms.

Herein, we established an NAFLD model by means of OVX in female rats and performed 16S rDNA amplicon sequencing of the gut microbiota and transcriptomics and metabolomics of liver tissue. This study aimed to comprehensively investigate the role of the linoleic acid (LA) metabolism pathway in the preventive effects of E_2 supplementation on NAFLD, particularly in surgically menopausal female rats. By employing a multidisciplinary approach combining in vivo and in vitro analyses, the study seeks to elucidate the mechanisms underlying the preventive effects of E_2 on NAFLD, focusing on its modulation of gut microbiota composition and liver metabolism and exploring the associations between E_2 supplementation, gut microbiota disturbance, and alterations in LA metabolism, with the ultimate goal of identifying potential targets for postmenopausal interventions in NAFLD treatment.

2. Materials and methods

2.1. Animal

The study protocol conformed to the ARRIVE guidelines [15] and the National Research Council's Guide for the Care and Use of Laboratory Animals [16]. The protocol was approved by the Committee of Animal Experimentation (MDKN-2022-026). Eight-week-old female Sprague–Dawley (SD) rats weighing 180–190 g were purchased from Beijing Vital River Laboratory Animal Technology Co., Ltd. All rats had free access to food and water under specific pathogen-free conditions (12-h light/dark cycle). All rats had one week of acclimation before being subjected to the research protocols.

2.2. Research protocol

Divide the rats into three groups: sham group, OVX group, and estrogen supplementation treatment group. To induce anesthesia, rats were placed in an anesthesia induction box containing 4% isoflurane (R510-22, RWD) in an oxygen/air mixture. After that, 2% isoflurane was administered through an animal anesthesia machine (R530IE, RWD) to maintain anesthesia. Subsequently, OVX surgery was performed according to established protocols [17]. Rats in the sham group underwent the same procedure as the OVX group, except that they only underwent the removal of adipose tissue around the ovaries instead of bilateral ovary removal. Beginning on the day of surgery, 17β-estradiol (20 μg/kg/day, E8875, Sigma) or vehicle was injected subcutaneously every day for 8 weeks. Vaginal smears of 14 consecutive days were used to forecast the hormonal status and estrous cycle changes before and after surgery. The protocol conformed to previously reported protocols [18]. During the whole research period, the rats were checked daily, and their body weight was recorded weekly.

2.3. Histopathological analysis

Tissue samples of liver, subcutaneous fat, mesenteric adipose, perinephric fat and colon were fixed in 4% paraformaldehyde at 4 °C. After dehydration, paraffin immersion and embedding, samples were sectioned at a thickness of 4 μm for subsequent staining. Hematoxylin and eosin (H&E) staining was used for histological evaluation and adipocyte area analysis. Oil Red O staining was used to display hepatocyte steatosis in vivo and in vitro.

2.4. Blood biochemistry

Blood samples were collected from the abdominal aorta. Blood samples were incubated for one night at 4 °C and centrifuged at 3500 g/min for complete separation of serum, which was used in further biochemistry tests. Enzyme-linked immunosorbent assay (ELISA) was used to measure hormone levels, including E_2 (E-OSEL-R0001, Elabscience), luteinizing hormone (LH, E-EL-R0026c, Elabscience) and follicle-stimulating hormone (FSH, E-EL-R0391c, Elabscience). Preliminary experiments indicated that serum samples could be used directly for E_2 measurement, while 2-fold dilution and 6-fold dilution could be used for FSH and LH measurement. Other procedures were conducted following the kit instructions. A colorimetric method (single reagent) was used to measure glutamic oxalacetic transaminase (AST), glutamic-pyruvic transaminase (ALT), total cholesterol (TC), triglycerides (TG), high-density lipoprotein (HDL) and low-density lipoprotein (LDL) according to the kit instructions (BIOSINO).

2.5. Transmission electron microscopy (TEM)

Liver tissue and colon tissue were cut into 1 mm × 1 mm × 2 mm pieces. After prefixing, postfixing, dehydration, immersion and embedding, samples were cut into 70-nm sections. Double staining with uranyl acetate and lead citrate was employed for TEM observation and capture.

2.6. Immunofluorescent staining

Paraffin sections were routinely dewaxed, rehydrated, subjected to antigen recovery and blocked in turn. Recombinant anti-ZO1 tight junction antibody (1:150, ab221547, Abcam) was used as the primary antibody. The nuclear counterstain was DAPI (blue).

2.7. Fecal 16S rRNA gene sequencing

Fecal samples (500 mg) from the rectum were collected and stored at −80 °C. Genomic DNA extraction was conducted using a Magnetic Stool DNA Kit (DP712, TIANGEN). The purity and concentration of extracted DNA were determined by 1% agarose gel electrophoresis. The DNA samples were diluted to a final concentration of 1 ng/μL 16S rRNA genes of the V3–V4 regions were amplified. Thermal cycling was set as initial denaturation at 98 °C for 1 min; 30 cycles of denaturation at 98 °C for 10 s, annealing at 50 °C for 30 s, and elongation at 72 °C for 30 s; and 72 °C for 5 min. After identification by 2% agarose gel electrophoresis, qualified PCR products were purified and subjected to library preparation and sequencing. The Clean Tags sequence, aligned with the Silva database with a similarity cutoff of 97%, underwent further processing to detect and remove chimeric sequences, resulting in the derivation of the final effective tags. After denoising and filtering the effective tags, species annotation and phylogenetic relationship

construction were conducted using QIIME2 software. Data normalization was performed before analysis of alpha and beta diversity. Alpha diversity was calculated from 6 indices, namely, the Chao1, Observed_features, Dominance, Plelou_e, Shannon and Simpson indices. For beta diversity, principal coordinate analysis (PCoA) was performed to visualize differences among samples. Significantly different species at each taxonomic level (phylum, class, order, family, genus and species) were analyzed. Functional prediction was conducted by LEfSe analysis and exhibited by an LDA tree. Correlation heatmaps between species at each taxonomic level and other indicators, including blood biochemistry and metabolites, were generated by R software (4.3.0).

2.8. Transcriptome analysis

Liver samples were flash-frozen in liquid nitrogen and stored at −80 °C before sequencing. After RNA extraction quantification and qualification, the cDNA library consisted of 370~420 bp purified with the AMPure XP system (Beckman Coulter, Beverly, USA). The library preparations were sequenced on an Illumina NovaSeq platform, and 150-bp paired-end reads were generated. Clean data (clean reads) were obtained by removing reads containing adapters, reads containing poly-N and low-quality reads from the raw data. At the same time, the Q20, Q30 and GC contents of the clean data were calculated. All downstream analyses were based on clean data with high quality. After read mapping, featureCounts v1.5.0-p3 was used to count the read numbers mapped to each gene. Then, the FPKM of each gene was calculated based on the length of the gene and read count mapped to this gene. Differential expression analysis of each pair of groups was performed using the DESeq2 R package (1.20.0). Genes with an adjusted p value ≤ 0.05 were considered differentially expressed. Gene Ontology (GO) and KEGG enrichment analyses of differentially expressed genes were implemented by the clusterProfiler R package.

2.9. Untargeted Metabolomic

Tissue samples were ground with liquid nitrogen and resuspended in prechilled 80% methanol. After incubation and centrifugation, the supernatant was diluted to a final concentration containing 53% methanol by LC−MS grade water. Then, the samples were recentrifuged, and the supernatant was injected into the LC−MS/MS system for analysis. The raw data files generated by UHPLC−MS/MS were processed using Compound Discoverer 3.1 (CD3.1, Thermo Fisher) to perform peak alignment, peak picking, and quantitation for each metabolite. These metabolites were annotated using the KEGG database, HMDB and LIPIDMaps database. The metabolites with VIP >1 and p value < 0.05 and fold change ≥ 2 or FC ≤ 0.5 were considered differentially expressed metabolites.

2.10. Cell lines and treatment

The BRL 3A cell line (Rat, CL-0036, Pricella, CVCL-0606) was used for in vitro exploration. Cells were treated with vehicle, a mixture of palmitic acid and oleic acid (PA + OA, 245 μM + 122.5 μM) [19], gradient concentrations of linolic acid (LA, 50 μM, 100 μM, 200 μM, 300 μM and 400 μM) and/or E_2. A TG concentration colorimetric assay kit (E-BC-K261-M, Elabscience) was used to evaluate hepatocyte steatosis in cell lines.

2.11. Evaluation of cell death

The cell density was adjusted to 3×10^4 cells/mL in 100 μL/well in 96-well plates. After certain treatments, the Cell Counting Kit-8 (CCK-8, CK04, DoJinDo) assay was used for cell death determination. The working solution was added to the wells for 4 h of incubation and then measured using a microplate reader at 450 nm absorbance.

2.12. Quantitative Real-Time Polymerase Chain Reaction (qRT-PCR) analysis

The mRNA levels of Cyp3a9, Cyp1a2, Pla2g16 and Cyp3a18 in liver tissue or treated cells were determined by qRT−PCR analysis. The PCR primer information were reflected in Table 1. Total RNA extraction was conducted with TransZol (ET101, TransGen Biotech). Reverse transcription was performed by FastKing gDNA Dispelling RT SuperMix (KR118, TIANGEN Biotech). qRT−PCR was conducted

Table 1
PCR primer information.

Gene	PCR primer sequences
Rattus GAPDH_F	GCTGAGTATGTCGTGGAGTC
Rattus GAPDH_R	GATGCATTGCTGACAATCTT
Rattus CYP3A9_F	CACGGATCCAGACATAATCAA
Rattus CYP3A9_R	GATCCCTGCCTCATGTTTC
Rattus Pla2g16_F	ATGCCCATACCAGAACCC
Rattus Pla2g16_R	CGCTGGATGATCTTGTTCA
Rattus CYP3A18_F	AACCTTCACCAGTGGCAAA
Rattus CYP3A18_R	ATCGACGTTCACTCCAAATG
Rattus Cyp1a2_F	CCTTTGTCCCCTTCACCAT
Rattus Cyp1a2_R	TCACTCAGGGTCTTGTCGAT

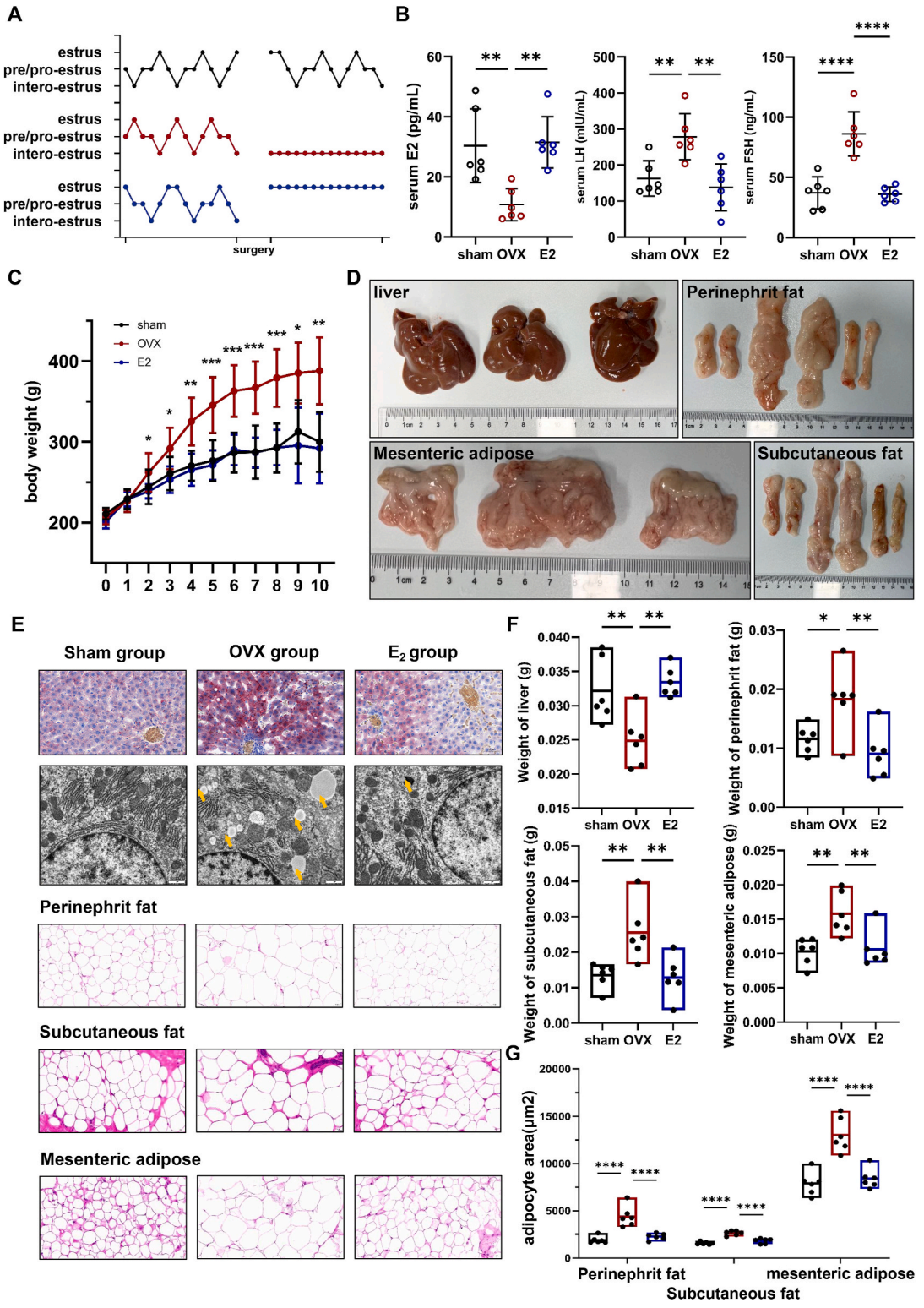

Fig. 1. Female rats developed excess weight gain and NAFLD after OVX. (A) Typical estrous cycle changes before and after modeling. (B) Measurement of serum hormones, including LH, FSH and E_2 (n = 6). (C) Weight gain of rats after modeling (n = 6). (D) Representative comparison photographs of liver, perinephric fat, mesenteric adipose and subcutaneous fat. (E) Representative images of Oil Red O staining of liver tissue (scale bar = 50 μm), lipid droplets under TEM of liver tissue (scale bar = 1 μm), H&E staining of perinephric fat, mesenteric adipose and subcutaneous fat (n = 6, scale bar = 20 μm). (F) Weight of the liver, perinephric fat, mesenteric adipose and subcutaneous fat. (G) Adiposity area analysis of the

perinephric fat, mesenteric adipose and subcutaneous fat (n = 6). (All error bars, mean values ± SD, p values were determined by unpaired two-tailed Student's *t*-test of n = 3 independent biological experiments. *p < 0.05; **p < 0.01; ***p < 0.001; ****p < 0.0001). (For interpretation of the references to color in this figure legend, the reader is referred to the Web version of this article.)

by TransStart® Top Green qPCR SuperMix (AQ131, TIANGEN Biotech). PCR primer sequences were designed using DNAMAN software and are listed as follows. The procedure for the amplification plot was set as 95 °C for 30 s and 55 °C for 20 s for 40 cycles in a 20-μl reaction system. The melt curve steps were 95 °C, 60 °C and 95 °C for 15 s each.

2.13. Statistical analysis

The data were collected and managed using Microsoft Excel 2019. Prior to conducting statistical analyses, the normality and homogeneity of variances of the data were assessed. For parametric tests, such as unpaired t-tests (two-tailed) for two-group comparisons and one-way analysis of variance (ANOVA) for multiple-group comparisons, normality and homogeneity of variances were confirmed. In the case of non-normally distributed data or heterogeneity of variances, appropriate non-parametric tests or transformations were applied. Multiple comparisons were adjusted using methods such as Bonferroni or Benjamini-Hochberg correction to mitigate the risk of Type I errors. Correlation analyses were conducted to explore the relationships between variables. Statistical analyses were performed using GraphPad Prism9 software. The significance levels were denoted as follows: *p < 0.05; **p < 0.01; ***p < 0.001; and ****p < 0.0001.

Correlation analyses were conducted to explore the relationships between variables. The methods employed for correlation analysis involved calculating Pearson's correlation coefficient for assessing linear relationships between continuous variables. Spearman's rank correlation coefficient was utilized to evaluate monotonic relationships between variables when the assumptions of Pearson's correlation were not met or when dealing with ordinal data. Correlation heatmaps, involved visualizing the relationships between variables through color-coded matrices. Correlation heatmaps provide a graphical representation of correlation coefficients between pairs of variables, with colors indicating the strength and direction of the correlations. Typically, correlation coefficients are computed using Pearson's correlation coefficient for linear relationships or Spearman's rank correlation coefficient for monotonic relationships. To create a correlation heatmap, the correlation coefficients are calculated for all pairs of variables in the dataset. These coefficients range from −1 to 1, where values close to 1 indicate a strong positive correlation, values close to −1 indicate a strong negative correlation, and values close to 0 indicate little to no correlation. The correlation matrix is then visualized as a heatmap, with colors ranging from cool tones (e.g., blue) for negative correlations to warm tones (e.g., red) for positive correlations.

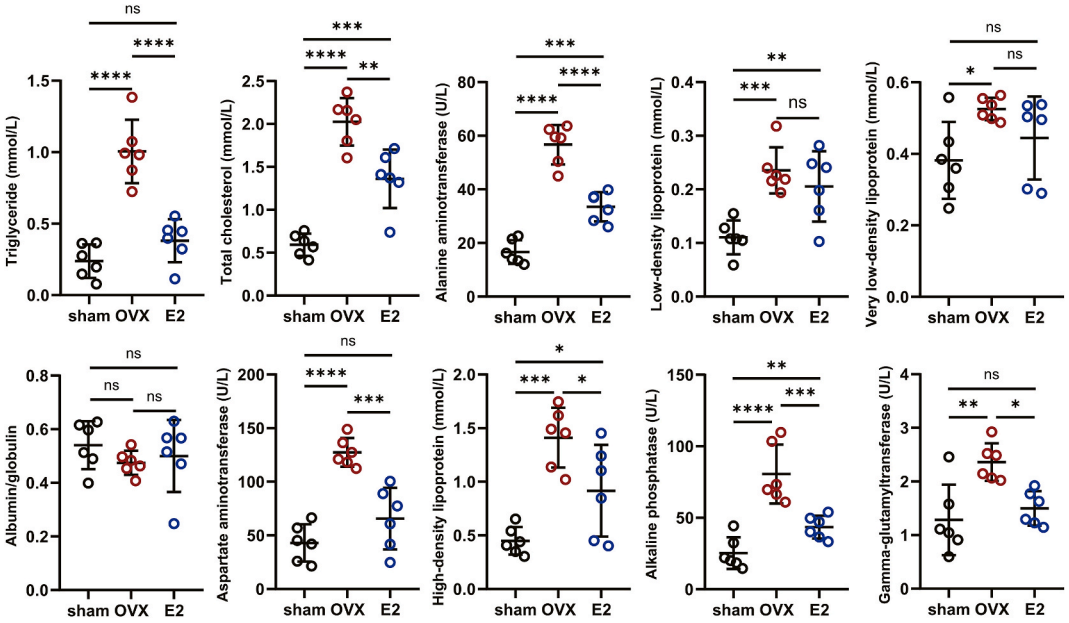

Fig. 2. Measurement of liver enzymes, blood lipids and lipoproteins (n = 6) (All error bars, mean values ± SD, p values were determined by unpaired two-tailed Student's *t*-test of n = 3 independent biological experiments. *p < 0.05; **p < 0.01; ***p < 0.001; ****p < 0.0001).

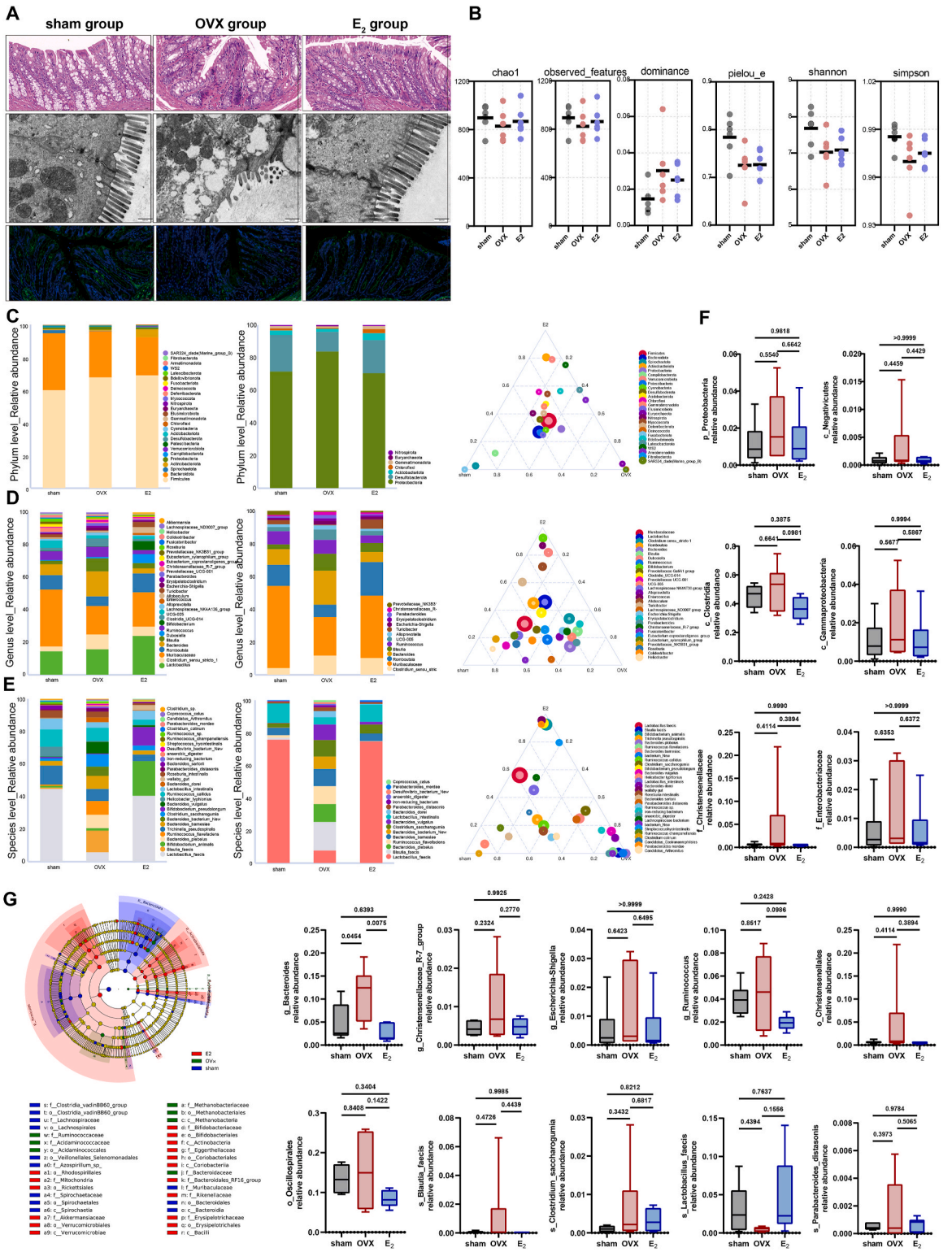

Fig. 3. Microbiome analysis of fecal samples in the sham group, OVX group and E_2 group. (A) Representative images of HE staining of colon tissue (scale bar = 50 μm), intestinal tight junctions under TEM (scale bar = 50 nm) and IF staining of ZO-1 (green, scale bar = 50 μm). (B) Alpha diversity analysis. (C) Stack diagram of the relative abundance of the top 26 phyla, key phyla and ternary phase diagram in the groups. (D) Stack diagram of the relative abundance of the top 30 genera, key genera and ternary phase diagram in the groups. (E) Stack diagram of the relative abundance of the top 30 species, key species and ternary phase diagram in the groups. (F) Box plots showing bacterial differences at different

classifications (n = 6). (G) LEfSe analysis (LDA threshold = 2). (All error bars, mean values ± SD, p values were determined by unpaired two-tailed Student's *t*-test of n = 3 independent biological experiments. *p < 0.05; **p < 0.01; ***p < 0.001; ****p < 0.0001). (For interpretation of the references to color in this figure legend, the reader is referred to the Web version of this article.)

3. Results

3.1. E_2 prevented female rats from developing NAFLD after OVX

A reproductive hormone deficiency model was established by OVX in female rats to simulate women who undergo surgical menopause or, to a certain extent, women after natural menopause. HRT in rats was performed by subcutaneous injection of E_2 (20 μg/kg/day). Two weeks after surgery, rats in the different groups developed typical changes in the estrous cycle, in which vaginal exfoliative cytology from rats in the OVX group showed continuous diestrus, while those from the E_2 group showed estrus (Fig. 1A). Serum levels of E_2, LH and FSH were as expected (Fig. 1B). These results confirmed the effect of hormone deficiency and HRT in the different groups.

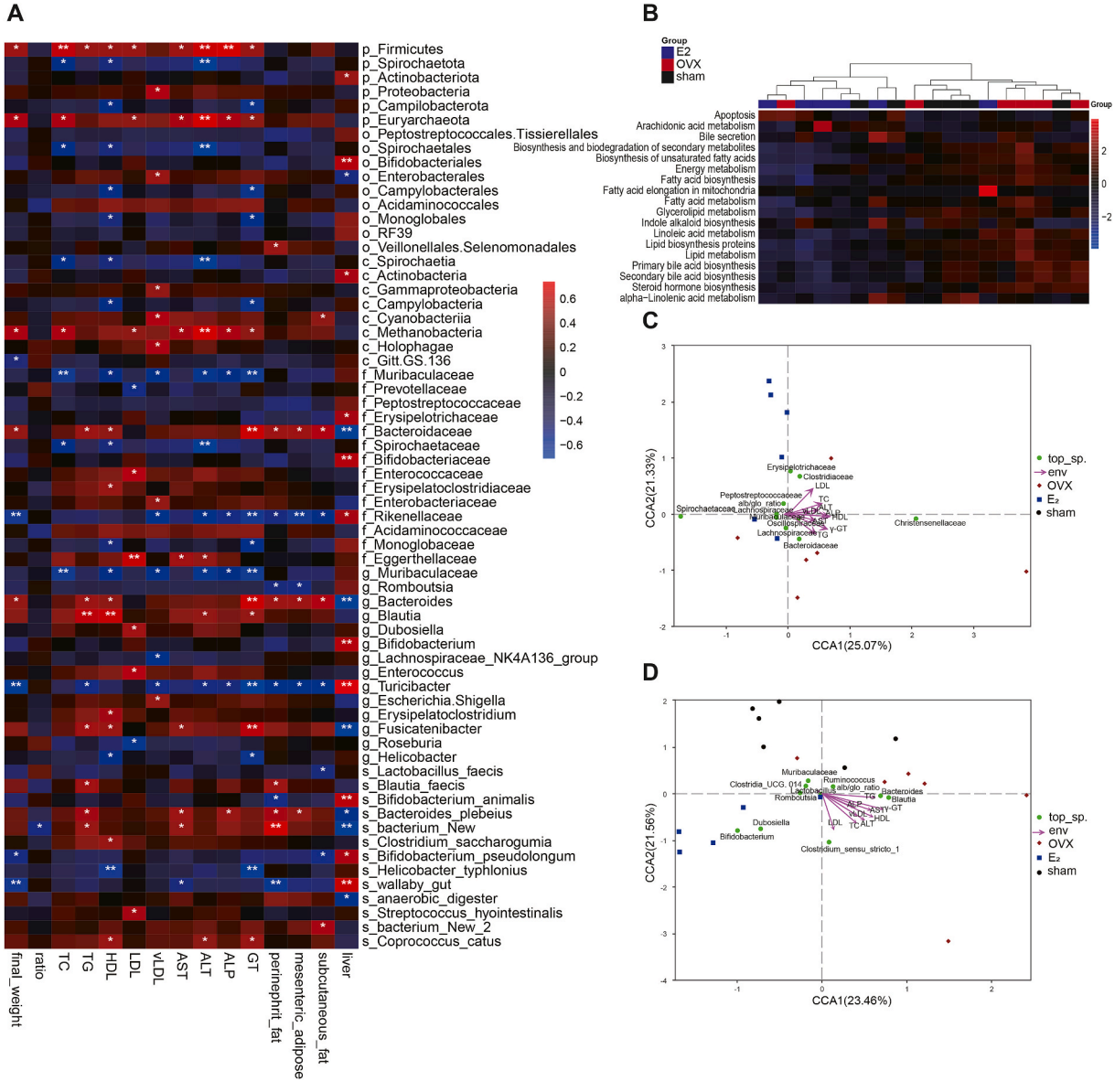

Fig. 4. Disturbance in the intestinal flora was related to clinical abnormalities in OVX-related NAFLD. (A) Correlation heatmap of the intestinal flora and clinical indicators. (B) PICRUSt analysis at level 3. (C) CCA analysis at the family level. (D) CCA analysis at the genus level.

Rats in the OVX group exhibited excess weight gain after surgery compared to that in the sham group, and this trend could be suppressed by E_2 supplementation (Fig. 1C). Then, the evaluation of gross anatomy and pathological analysis of liver and adipose tissue from various parts of the body revealed that rats in the OVX group developed NAFLD (Fig. 1D–G). Specifically, livers from the OVX group were lighter than those from the other two groups, while the perinephric fat, mesenteric adipose and subcutaneous fat were heavier (Fig. 1D–F). Oil Red O staining of liver tissue confirmed OVX-related NAFLD, which could be alleviated by E_2 supplementation. Lipid droplets were revealed by TEM (Fig. 1E). H&E staining indicated that loss of reproductive hormones caused excess fat accumulation in several areas of the body (Fig. 1E–G). There was no statistical difference among the groups in albumin/globulin ratio (Fig. 2). Abnormal serum lipids (TG and TC), lipoproteins (HDL, LDL and V-LDL) and liver enzymes (AST, ALT, ALP and GGT) suggested liver function injury (Fig. 2).

3.2. *OVX-related NAFLD was associated with an impaired intestinal barrier and altered gut microbiota*

The OVX group developed NAFLD accompanied by an impaired intestinal barrier, as revealed by morphological changes in the intestinal villi, damaged intestinal tight junctions, and decreased expression of ZO-1 (Fig. 3A). Thus, gut microbiota dysbiosis seemed reasonable (Fig. 3 and Supplementary Fig. 1). The alpha diversity was not apparently changed among the groups (Fig. 3B). The relative abundances at all levels were altered, and the ternary plot clearly showed the species distribution and evenness among the groups

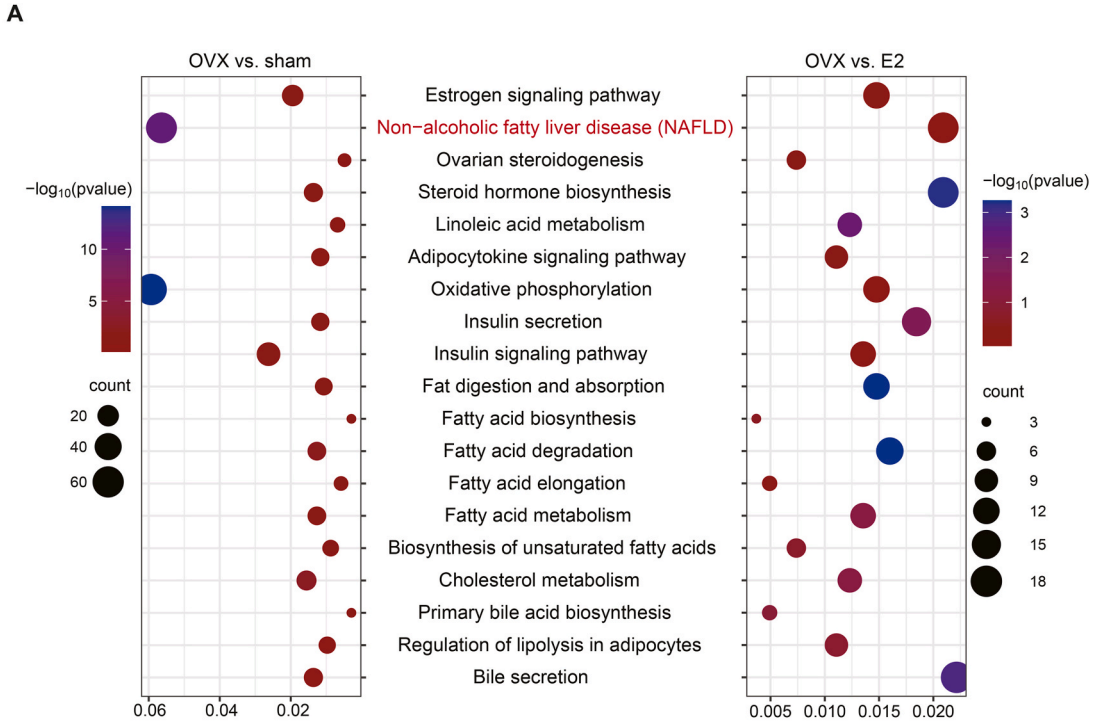

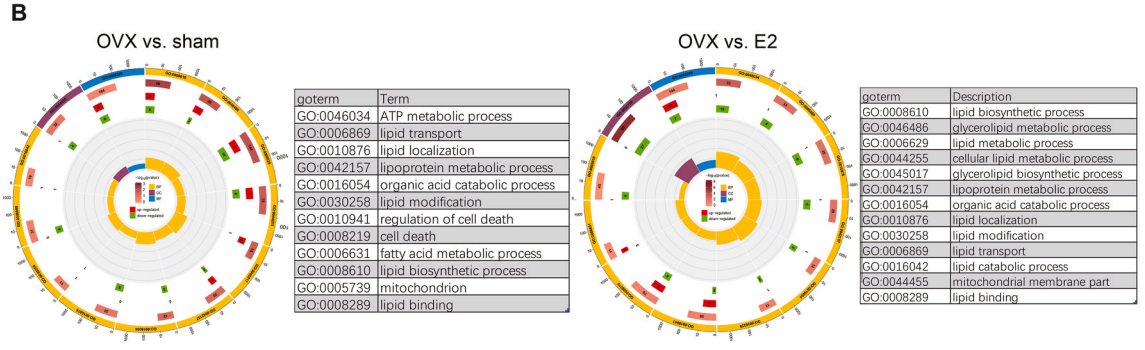

goterm	Term
GO:0046034	ATP metabolic process
GO:0006869	lipid transport
GO:0010876	lipid localization
GO:0042157	lipoprotein metabolic process
GO:0016054	organic acid catabolic process
GO:0030258	lipid modification
GO:0010941	regulation of cell death
GO:0008219	cell death
GO:0006631	fatty acid metabolic process
GO:0008610	lipid biosynthetic process
GO:0005739	mitochondrion
GO:0008289	lipid binding

goterm	Description
GO:0008610	lipid biosynthetic process
GO:0046486	glycerolipid metabolic process
GO:0006629	lipid metabolic process
GO:0044255	cellular lipid metabolic process
GO:0045017	glycerolipid biosynthetic process
GO:0042157	lipoprotein metabolic process
GO:0016054	organic acid catabolic process
GO:0010876	lipid localization
GO:0030258	lipid modification
GO:0006869	lipid transport
GO:0016042	lipid catabolic process
GO:0044455	mitochondrial membrane part
GO:0008289	lipid binding

Fig. 5. Transcriptomic analysis of liver tissue in the sham group, OVX group and E_2 group. (A) Double bar plot of KEGG pathway enrichment showing the shared pathways from the OVX group vs. the E_2 group and the OVX group vs. the sham group. (B) Loop graph of GO enrichment showing pathways from the OVX group vs. the E_2 group and the OVX group vs. the sham group.

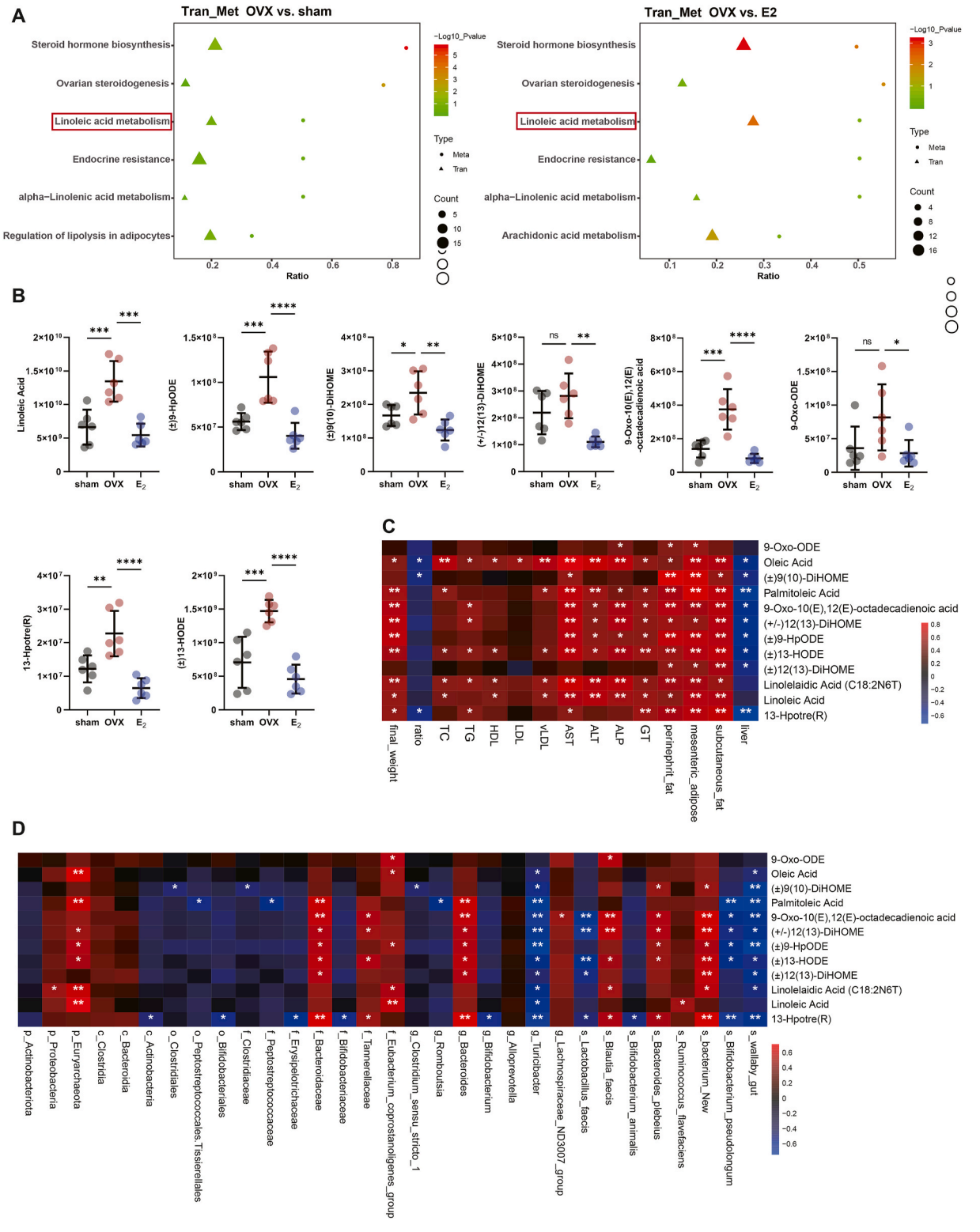

(caption on next page)

Fig. 6. Metabonomic analysis of liver tissue in the sham group, OVX group and E_2 group. (A) Coenrichment KEGG pathways of transcriptomic and metabonomic analysis in both the OVX group vs. the E_2 group and the OVX group vs. the sham group comparisons. (B) Differentially expressed metabolites in the linoleic acid metabolism pathway. (C) Correlation heatmap of clinical indicators and the relevant differentially expressed metabolites. (D) Correlation heatmap of the intestinal flora and the relevant differentially expressed metabolites. (All error bars, mean values ± SD, p values were determined by unpaired two-tailed Student's *t*-test of n = 3 independent biological experiments. *p < 0.05; **p < 0.01; ***p < 0.001; ****p < 0.0001).

(Fig. 3C–E, Supplementary Figs. 1B–G and Fig. 2A and B). We tried to select species that were potentially associated with E_2 levels and NAFLD (Fig. 3F and Supplementary Fig. 3H). At the phylum level, the relative abundance of *Proteobacteria* was higher in the OVX group than in the sham group and the E_2 group. At the class level, the OVX group had increased *Negativicutes*, *Clostridia* and *Gammaproteobacteria* abundances compared with those in the other two groups. At the family level, the abundances of *Christensenellaceae*, *Enterobacteriaceae*, *Bacteroidaceae*, *Butyricicoccaceae* and *Tannerellaceae* were increased, while those of *Muribaculaceae* and *Peptostreptococcaceae* were decreased in the OVX group. At the order level, increased levels of *Christensenellales*, *Oscillospirales* and *Enterobacterales* were observed in the OVX group, which were opposite to the trends in the sham and E_2 groups. At the genus level, the *Bacteroides*, *Christensenellaceae_R-7_group*, *Escherichia-Shigella*, *Ruminococcus*, *Erysipelatoclostridium*, *Parabacteroides*, *UCG-005* and *Blautia* abundances were higher in the OVX group, while the abundances of *Muribaculaceae*, *Turicibacter* and *Romboutsia* were lower. At the species level, the OVX group exhibited higher abundances of *Blautia_faecis*, *Clostridium_saccharogumia*, *Parabacteroides_distasonis*, *Bacteroides_barnesiae* and *Ruminococcus_flavefacies* and a lower abundance of *Lactobacillus_faecis*. Furthermore, LEfSe, which concentrates on both statistical significance and biological relevance, was performed to show the different species among groups and their evolutionary relationships on the species evolution branch map (Fig. 3G and Supplementary Figs. 2I and J).

After elucidating the different species at each level, the potential correlations between the different species and clinical indicators (final body weight, serum biochemistry indicators, weight of liver and adiposity from different body positions) were investigated. As shown in the correlation heatmap, p_Firmicutes, p_Euryarchaeota, c_Methanobacteria, f_Bacteroidaceae, g_Bacteroides, g_Blautia and s_Bacteroides_plebeius were positively associated with most clinical indicators, while p_Spirochaetota, o_Spirochaetales, c_Spirochaetia, f_Muribaculaceae, f_Spirochaetaceae, f_Rikenellaceae, g_Muribaculaceae and g_ Turicibacter were negatively associated with these indicators (Fig. 4A and Supplementary Figs. 2C–H). PICRUSt analysis provided a cluster heatmap of the predicted KEGG pathways and samples (Fig. 4B). The gut microbiota from the OVX group had different metabolic states compared with those from the sham and E_2 groups, including biosynthesis of unsaturated fatty acids, fatty acid biosynthesis, fatty acid biosynthesis metabolism, LA metabolism and lipid metabolism. CCA analysis directly showed the relationship among samples, environmental factors (serum biochemistry indicators) and the gut microbiota at the family and genus levels (Fig. 4C and D).

3.3. Bioinformatics analysis revealed the linoleic acid metabolism pathway as a vital change in vivo

Bioinformatics analysis from liver tissue contributed more to interpreting the functional changes. KEGG enrichment from transcriptomics analysis indicated that numerous pathways that were altered by OVX surgery were partially recovered by E_2 supplementation, including the estrogen signaling pathway, nonalcoholic fatty liver disease, LA metabolism, insulin signaling pathway and metabolism pathways related to fatty acids (Fig. 5A). GO enrichment focused more on different processes related to lipid metabolism (Fig. 5B). These data suggested that E_2 supplementation protected OVX rats from developing NAFLD. Liver metabolism was also changed simultaneously with NAFLD development and E_2 treatment (Supplementary Figs. 3 and 4). The combination of transcriptomics and metabonomics analysis highlighted that LA metabolism was enriched in comparisons of OVX vs. sham and OVX vs. E_2 (Fig. 6A). The liver LA content was significantly increased in the OVX group compared to the sham and E_2 groups, as were other metabolites in the LA metabolism pathway (Fig. 6B). These metabolites were closely related to abnormalities in clinical indicators (Fig. 6C). Gut microbiota alterations, including increased abundances of p_Euryarchaeota, f_Bacteroidaceae, f_Tannerellaceae, f_Eubacterium_coprostanoligenes_group, g_Bacteroides, s_Blautia_faecis, s_Bacteroides_plebeius and s_bacterium_New, as well as decreased abundances of g_Turicibacter, s_Lactobacillus_faecis, s_Bifidobacterium_pseudolongum and s_wallaby_gut, were obviously associated with high levels of liver LA and related metabolites (Fig. 6D and Supplementary Fig. 5). Bioinformatics analysis revealed that the LA metabolism pathway was vital in OVX-induced NAFLD, which was related to gut microbiota alterations and E_2 supplementation.

3.4. E_2 prevented linoleic acid-induced hepatic steatosis in vitro

More information is needed to elucidate the role of the altered LA metabolism in OVX-induced NAFLD. The mRNA levels of Cyp1a2, Cyp3a9, Pla2g16 and Cyp3a18 in liver tissue were changed as OVX-induced NAFLD appeared and were recovered with E_2 supplementation (Fig. 7A). These data confirmed the existence of altered LA metabolism. Next, we aimed to explore whether excess LA is able to induce hepatic steatosis in vitro. We performed an in vitro study using the BRL 3A cell line and compared it with the PA + OA protocol [19]. Data from BRL 3A cells showed that PA + OA caused significantly increased cell death accompanied by increased levels of TG accumulation at both incubation time points (Fig. 7B and C), and Oil Red O staining confirmed hepatocyte lipid deposition (Fig. 4D). For LA, cells treated with LA at 50 μM, 100 μM and 200 μM all survived with similar cell viability to that of the control group (Fig. 7B), while those treated with 200 μM LA developed significant TG accumulation compared with that in the control group (Fig. 7C). At 300 μM LA, cell viability was dramatically decreased, followed by a similar TG accumulation level induced by 200 μM LA.

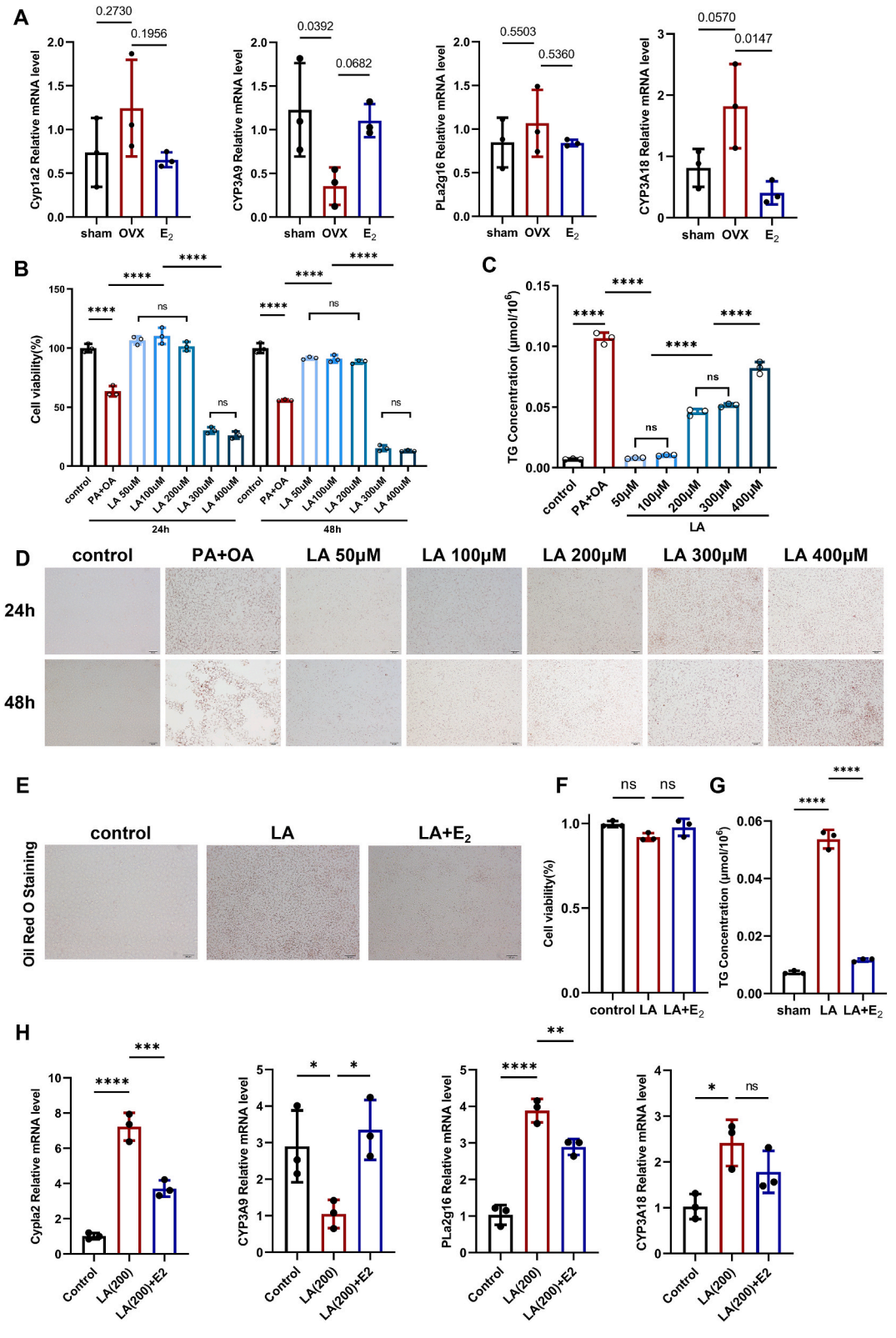

(caption on next page)

Fig. 7. E_2 inhibits LA-induced hepatocyte steatosis in vitro. (A) Relative RNA levels of Cyp1a2, CYP3A9, PLa2g16 and CYP3A18 in liver tissue (n = 3). (B) Cell viability of BRL 3A cells treated with PA + OA or gradient concentrations of LA for 24/48 h (n = 3). (C) TG concentration of BRL 3A cells treated with PA + OA or gradient concentrations of LA for 48 h (n = 3). (D) Representative images of Oil Red O staining (n = 3, scale bar = 50 μm) of BRL 3A cells treated with PA + OA or gradient concentrations of LA for 24 h (upper panel) and 48 h (lower panel). (E) Representative images of Oil Red O staining of the BRL 3A cell line under treatment with LA (200 μM) and/or E_2 (0.1 μM) for 48 h. (F) Cell viability of BRL 3A cells (n = 3). (G) TG concentration of BRL 3A cells (n = 3). (H) Relative RNA levels of Cyp1a2, CYP3A9, PLa2g16 and CYP3A18 in BRL 3A cells (n = 3). (All error bars, mean values ± SD, p values were determined by unpaired two-tailed Student's *t*-test of n = 3 independent biological experiments. *$p < 0.05$; **$p < 0.01$; ***$p < 0.001$; ****$p < 0.0001$). (For interpretation of the references to color in this figure legend, the reader is referred to the Web version of this article.)

Treatment with 400 μM LA had similar cytotoxicity to hepatocytes as treatment with 300 μM LA but excellent inducing capacity (Fig. 7B–C). We chased 200 μM LA for exploration because it could induce hepatic steatosis without excess cell death, which was similar to that observed in OVX-induced NAFLD, an early stage of hepatic steatosis (Fig. 7D). E_2 treatment, to a great extent, diminished hepatic steatosis induced by LA (Fig. 7E–G). Moreover, the mRNA levels of Cyp1a2, Cyp3a9, Pla2g16 and Cyp3a18 in treated cells were as expected (Fig. 7H). The in vitro study supported the results from the in vivo study that abnormal LA metabolism caused OVX-induced NAFLD, which could benefit from E_2 supplementation.

4. Discussion

The present research focused on a special type of NAFLD that was induced by OVX, simulating women who undergo surgical menopause. The model was established by removal of the bilateral ovaries. Eight weeks after surgery, rats exhibited excess weight gain, and pathological analysis and serum biochemical indicators demonstrated the existence of NAFLD, which could be diminished by E_2 supplementation. Fecal 16S rRNA gene sequencing showed alterations in the gut microbiota during this period. The combination of metabolomics and transcriptomics jointly revealed enrichment of the LA metabolism pathway, which was not previously mentioned in OVX-induced NAFLD. The gut microbiota was closely associated with serum biochemical indicators and different metabolites in the LA metabolism pathway. Then, we performed an in vitro study and proved that LA could induce hepatic steatosis. E_2 treatment protected OVX rats from NAFLD and LA-induced cells from hepatic steatosis, likely by changing LA metabolism.

Dietary manipulation models are more commonly used in this field, including the methionine- and choline-deficient (MCD) diet or a choline-deficient, L-amino acid-defined diet, high-fat diet (HFD) and high-cholesterol diet. NAFLD tends to be a metabolic disease with multiple stages and factors, which means that personalized and effective disease management should strive to consider more of those factors. Surgical or natural menopause-related reproductive hormone deficiency is associated with a high risk of NAFLD and is one of the targeted populations for active interventions [6]. Reduced estrogen levels in postmenopausal women promote changes in the levels of numerous lipids (lipoproteins, apolipoproteins, and triacylglycerols) circulating in the blood, thus triggering impaired lipid metabolism in the body [20]. Several investigations have demonstrated that estrogen not only modulates hepatic cholesterol uptake and reverses cholesterol transport [21] but also regulates cholesterol production [22] in the liver. Sex differences must be considered regarding NAFLD management, and sex-specific interventions are nonnegligible [23]. Our data provided evidence for HRT use in preventing NAFLD. The mechanisms by which E_2 exerts its metabolic protective effects, such as preventing NAFLD, lack adequate attention and research.

The interaction between liver disease and gut dysbiosis is a concern in both basic and clinical research [24]. Recent studies on the NAFLD-related gut microbiota changes have focused primarily on plant compounds, pharmaceutical ingredients or probiotics and prebiotics that may potentially reverse liver steatosis, such as CM3-SII polysaccharide [25], flavonoids contained in Citri Reticulatae Pericarpium [26], fucoxanthin [27], flaxseed [28], phytosterols [29], isoquercetin [30], NUTRIOSE® soluble fiber [31]. The gut microbiota shows distinct diversity in subjects of reproductive age but is not so different after menopause between males and females [32]. E_2 supplementation is extensively used to address reproductive hormone deficiency-related symptoms in the clinic, and during this period, women are potentially able to regain the protective effects of E_2 against metabolic diseases. Thus, instead of painstakingly searching for effective treatments, perhaps we can focus some attention on this established intervention to address multiple purposes. Data connecting E_2 supplementation in OVX-induced NAFLD and the gut microbiota are scarce. Damage to the gut barrier during the process of NAFLD after OVX was observed through TEM and immunofluorescence and was undoubtedly related to the gut microbiota disturbance. This was consistent with a previous report that E_2 improved intestinal barrier function and manifested a higher anti-inflammatory response in mice [33,34]. Our research indicated that E_2 supplementation potentially recovered some of the altered microbes associated with NAFLD indicators.

The *Proteobacteria* phylum exhibited a highly increased prevalence, which is a potential diagnostic signature of dysbiosis and a risk factor for many metabolic diseases [35], and instead of *Bacteroidetes* and *Firmicutes*, it could explain the significant functional variability in the human gut microbiota [36]. *Proteobacteria* were consistently enriched in human steatosis and nonalcoholic steatohepatitis [11]. This high-level enrichment was also observed in OVX-induced NAFLD rats. The relative abundance of the class *Gammaproteobacteria* was increased during the progression of alcoholic liver disease [37], and we found that it tended to increase in OVX-induced NAFLD in rats. *Clostridia* and *Negativicutes* were more abundant in obese type 2 diabetes mellitus (T2DM) patients [38] as well as gestational diabetes mellitus patients [39]. Similar to our OVX-induced NAFLD model, the abundance of *Clostridia* was increased, as it may be associated with multiple metabolism disorders. However, the class *Clostridia* plays a conflicting role because it was found to have a decreased abundance in NAFLD progression induced by a Western diet [40]. At the family level, the enrichment of *Enterobacteriaceae* induced by a HFD has been correlated with impaired glucose homeostasis [41] and was herein associated with

OVX-induced NAFLD. The genus *Parabacteroides* content was reported to be lower in postmenopausal than in premenopausal women [42], yet we found it to be higher in the OVX group, and other research has reported that *Parabacteroides* was enriched in early hepatocellular carcinoma (HCC) [43]. The *Bacteroides* genus is also thought to have an indeterminate role in NAFLD due to both increased [44] and decreased [45] levels. In our OVX-induced NAFLD model, the level of *Bacteroides* was significantly increased in the model group without intervention. These altered microbes remained stable when E_2 supplementation was appropriate. The results from our research indicated that E_2 supplementation contributed to preventing OVX-induced NAFLD with respect to the gut microbiota. In addition, it is even more exciting that the relationship wherein the gut microbiota is influenced by estrogens or other hormones is not unidirectional or passive [46]. The name "estrobolome" defines a group of genes in the gut microbiota that encode enzymes that are able to metabolize estrogen and are regulated by estrogen at the same time [47]. Data from human volunteers indicated that the gut microbiota affects systemic estrogen levels [48]. The gut microbiota has the potential to manipulate the metabolism of phytoestrogens such as the soy isoflavone daidzein and to strengthen their benefits [49]. These interactions make it more difficult to elucidate the functional influences that occur in both directions. As previously reported, 17β-hydroxysteroid dehydrogenases [50], the α1 subunit of Na^+/K^+-ATPase [51], carnitine palmitoyltransferase-II [52] and other targets are involved in those mechanisms. Functional validations are required to determine the role of microbes and their interactions with the host.

LA is considered an essential fatty acid from n-6 polyunsaturated fatty acids with many health benefits [53]. Absolute lack of LA causes essential fatty acid deficiency [54]. As a normal healthy diet can meet the requirement, LA is not commonly supplemented separately. To date, evidence tends to suggest that there should be an appropriate range for LA intake [55]. High serum concentrations of LA seem to be a protective factor associated with low odds for future NAFLD and cardiovascular risk, as reported in Finnish adults [56,57]. These results appear to conflict with those of the present study. Notably, the metabolism and biological function of fatty acids were different between men and women. Whether LA intake and the LA concentration in serum and tissue parallel each other and whether the serum LA level and liver tissue LA level are consist need more information. The controversial role of LA in metabolic disorder was not first noticed here. An earlier study on adipose tissue from different body sites of obese patients indicated that central obesity was positively associated with n-6 polyunsaturated fatty acids in adipose tissue [58]. Data from the Heidelberg cohort, which enrolled 9,182 men and 10,867 women with a 6.5-year follow-up, found that LA intake greater than 10.9 g/day was associated with large weight gain in normal-weight males, and LA intake greater than 11.2 g/day was associated with excess weight gain regardless of baseline body weight [59]. Subsequently, the Sydney Diet Heart Study was designed as a single-blinded, parallel group, randomized controlled trial and revealed that replacing dietary saturated fat with LA significantly reduced serum TC but increased the rates of death from all causes, coronary heart disease, and cardiovascular disease [60]. Recent studies using rodent models might help explain these conflicting results. In a rat model of essential fatty acid deficiency, an appropriate ratio of LA:alpha-linolenic acid (ALA, representing n-6/n-3 polyunsaturated fatty acids) could diminish symptoms caused by deficiency, but this benefit was weakened when the LA:ALA ratio was too high [61]. This calls attention to the fact that not only meeting the necessity of certain fatty acids but also controlling an appropriate proportion of intake is essential. Excess LA may cause the accumulation of reactive oxygen species (ROS) through its uncontrolled metabolites [62]. Even in the progression of NAFLD to HCC, LA was considered to disrupt mitochondrial function, cause more oxidative damage, mediate selective loss of intrahepatic CD4 (+) T lymphocytes and contribute to NAFLD-promoted HCC in both humans and mice [63]. In our opinion, the importance of LA in human health needs to be reconsidered carefully. Conflicting results regarding the data available highlight the potential harmful effect of LA, which should be more rigorously validated.

E_2 supplementation was able to sustain the transcription of lipid metabolism genes and then to protect female rats from changes in the proportions of fatty acids after OVX [64]. Our research highlighted the role of altered LA metabolism in OVX-induced NAFLD, which was also accompanied by related changes at the transcriptional level. In vitro and in vivo studies both found increased Cyp1a2, Pla2g16 and Cyp3a18 as well as decreased Cyp3a9 at the mRNA level. These differences caused by OVX could be kept unchanged by E_2 supplementation. Liver CYP1A2, CYP3A and CYP4A1 demonstrated high expression at the protein expression level in females [65]. Sex-specific differences in P450 enzyme levels are of great importance for understanding the differences between males and females in disease occurrence, development and treatment outcomes [64,66]. Multiple human studies have shown increased expression levels of hepatic CYP3A4, which lead to higher clearance rates of CYP3A4 substrates in women than in men [67]. Correspondingly, there are higher clearance rates of CYP1A2, CYP2E1, and CYP2D6 substrates in men than in women [68]. This sex difference also exists in rats. That is, CYP3A18 is a male-specific form, while CYP3A9 is a female-dominant form [69]. In our OVX-induced NAFLD model, Cyp3a9 was downregulated. Similar to patients with NAFLD, the activity of CYP3A4 was decreased at both the mRNA and protein levels [70]. E_2 treatment promoted Cyp3a9 mRNA expression not only in our research [71]. The expression level of Cyp1a2 was not entirely consistent between C57BL/6 mice and ob/ob mice [72]. The results from ob/ob mouse models showed that the mRNA expression, protein level, and activity of Cyp1a2 were significantly decreased [73], and the same changes could be seen in HFD-induced obese rats [74]. In contrast, C57BL/6 mice fed a HFD showed upregulated Cyp1a2 expression [75]. We hypothesized that Cyp1a2 was upregulated in OVX-induced NAFLD. Research on PLA2G16 has mainly focused on adipose tissue due to its capacity to regulate adipocyte lipolysis and promote obesity. PLA2G16 has been identified as one of the downstream effectors of PPARγ involved in adipogenesis [76]. Regulation of adipose tissue lipolysis might be a process by which PLA2G16 regulates PGE2 levels in an autocrine/paracrine manner through the PGE2/EP3/cAMP pathway [77]. Other roles of PLA2G16 include insulin resistance [78], RAS suppression [79], organelle degradation [80], colorectal cancer [81], pan-enterovirus host factor [82] and peroxisome biogenesis [83]. However, the function of PLA2G16 in the liver has not yet been reported. Based on its close relationship with OVX-induced NAFLD reported in our research and its wide effects, PLA2G16 should be further explored in this field.

It cannot be ignored that rodent models possess inevitable differences from humans in the specific pathophysiology of disease. Phenotypic or pathological similarity does not mean that basic research could be completely translated to humans, especially in

diseases with multiple pathogeneses. Further data from women with reproductive hormone deficiency are needed. In research conducted for observational study or functional validation, the names of microbes are not unified. Different names for microbes might limit cross-comparisons in the data pool. More importantly, different microbes from different species, such as humans and rats, can have similar functions, which needs more exploration. Our research did not involve separate studies of different levels of E_2 in the circulation, liver or locally in the intestine, which we thought could establish a better understanding of the relationships described in this article. NAFLD has been studied for more than 40 years, and we still do not understand it well and have not established an effective treatment system. Experts have suggested that NAFLD might not be an optimal name for this disease. The name "metabolic (dysfunction)-associated fatty liver disease (MAFLD)" may be more suitable for its complicated characteristics and may promote the establishment of a subphenotype system of the disease to accelerate the translational path to new treatments [2]. Certainly, there are some who do not support the update. In our view, surgical or natural menopause is, to be exact, an endocrine hit for women in their life accompanied by systemic metabolic changes. NAFLD is only one of those manifestations that is not limited to a "nonalcoholic" basis. We think that the name "MAFLD" brings with it an attitude that disease treatment and research should be more individualized.

5. Conclusion

This article reports the association among the gut microbiota, liver metabolism and liver transcription in OVX-induced NAFLD. The analysis of the gut microbiome revealed noteworthy abnormalities in key metabolic pathways related to unsaturated fatty acids, as well as fatty acid biosynthesis and metabolism, within the OVX group. Specifically, dysregulation was observed in the biosynthesis of unsaturated fatty acids and the metabolic processes associated with fatty acid synthesis in the gut microbiota of OVX-induced NAFLD rats.

Furthermore, analysis of liver metabolism and transcription unveiled a predominant aberration in LA metabolism in OVX group, signifying its pivotal role in the observed fatty acid metabolic disturbances in liver. This finding suggests that the dysregulated metabolism of LA may contribute significantly to lipid metabolism abnormalities in the pathogenesis of postmenopausal NAFLD. The metabolic disorder of LA may also have an impact on the lipid metabolism disorder of the intestinal microbiota. The metabolic perturbations of LA may directly and secondhandly impacting the development of NAFLD in postmenopausal individuals.

Importantly, the administration of E_2 demonstrated promising outcomes in ameliorating LA-induced fatty liver, and also evidenced by improvements in both microbial composition and fatty acid metabolism parameters observed in the E_2 treatment group. These findings suggest that E_2 exerts a dual effect, directly mitigating LA-induced liver pathology and indirectly modulating gut microbiota composition to prevent the onset of postmenopausal NAFLD.

In conclusion, our results highlight the interconnectedness between gut microbiota dysbiosis, aberrant fatty acid metabolism, and the protective effects of E_2 supplementation in postmenopausal NAFLD. By elucidating these complex interactions, our study provides valuable insights into the underlying mechanisms of NAFLD development and contributes more understanding about sex difference in NAFLD, also underscores the potential of hormone replacement therapy as a therapeutic strategy for preventing and managing postmenopausal NAFLD.

Funding

This study was supported by grant from the National High Level Hospital Clinical Research Funding (2022-PUMCH-C-065).

Availability of data and materials

The dataset(s) supporting the conclusions of this article are included within the article and its additional files.

Ethics statement

This study was approved by the Committee on the Ethics of Animal Experiments of the Peking Union Medical College Hospital (MDKN-2022-026).

CRediT authorship contribution statement

Ying Tian: Writing – review & editing, Writing – original draft, Data curation. **Yuan Xie:** Software, Methodology. **Xinyu Hong:** Visualization, Project administration, Methodology. **Zaixin Guo:** Project administration, Methodology. **Qi Yu:** Supervision, Project administration, Investigation, Data curation.

Declaration of competing interest

The authors declare that they have no known competing financial interests or personal relationships that could have appeared to influence the work reported in this paper.

Data availability

The raw data had been uploaded to the public database with accession number of PRJNA1089589 and PRJNA1088774. The website address for accessing the data is http://www.ncbi.nlm.nih.gov/bioproject/1089589 and https://www.ncbi.nlm.nih.gov/sra/PRJNA1088774.

Acknowledgements

Thanks to the Public laboratory platform and Cell Biology Core Facility of National Science and Technology Key Infrastructure on Translational Medicine in Peking Union Medical College Hospital for assistance with the instruments in this research.

Appendix A. Supplementary data

Supplementary data to this article can be found online at https://doi.org/10.1016/j.heliyon.2024.e29013.

References

[1] Z.M. Younossi, et al., The global epidemiology of nonalcoholic fatty liver disease (NAFLD) and nonalcoholic steatohepatitis (NASH): a systematic review, Hepatology 77 (4) (2023) 1335–1347, https://doi.org/10.1097/hep.0000000000000004.
[2] M. Eslam, A.J. Sanyal, J. George, MAFLD: a Consensus-driven proposed nomenclature for metabolic associated fatty liver disease, Gastroenterology 158 (7) (2020) 1999–2014.e1, https://doi.org/10.1053/j.gastro.2019.11.312.
[3] A. Santos-Laso, et al., Pathophysiological mechanisms in non-alcoholic fatty liver disease: from drivers to targets, Biomedicines 10 (1) (2021), https://doi.org/10.3390/biomedicines10010046.
[4] J.S. Klair, et al., A longer duration of estrogen deficiency increases fibrosis risk among postmenopausal women with nonalcoholic fatty liver disease, Hepatology 64 (1) (2016) 85–91, https://doi.org/10.1002/hep.28514.
[5] A.A. Florio, et al., Oophorectomy and risk of non-alcoholic fatty liver disease and primary liver cancer in the Clinical Practice Research Datalink, Eur. J. Epidemiol. 34 (9) (2019) 871–878, https://doi.org/10.1007/s10654-019-00526-1.
[6] K. Wegermann, et al., Tackling nonalcoholic fatty liver disease: three targeted populations, Hepatology 73 (3) (2021) 1199–1206, https://doi.org/10.1002/hep.31533.
[7] M. Grossmann, et al., Reproductive endocrinology of nonalcoholic fatty liver disease, Endocr. Rev. 40 (2) (2019) 417–446, https://doi.org/10.1210/er.2018-00158.
[8] Z.C. Zhang, et al., Upregulation of miR-125b by estrogen protects against non-alcoholic fatty liver in female mice, J. Hepatol. 63 (6) (2015) 1466–1475, https://doi.org/10.1016/j.jhep.2015.07.037.
[9] B.M. Galmés-Pascual, et al., 17β-estradiol ameliorates lipotoxicity-induced hepatic mitochondrial oxidative stress and insulin resistance, Free Radic. Biol. Med. 150 (2020) 148–160, https://doi.org/10.1016/j.freeradbiomed.2020.02.016.
[10] A. Besse-Patin, et al., Estrogen signals through peroxisome proliferator-activated receptor-γ coactivator 1α to reduce oxidative damage associated with diet-induced fatty liver disease, Gastroenterology 152 (1) (2017) 243–256, https://doi.org/10.1053/j.gastro.2016.09.017.
[11] J. Aron-Wisnewsky, et al., Gut microbiota and human NAFLD: disentangling microbial signatures from metabolic disorders, Nat. Rev. Gastroenterol. Hepatol. 17 (5) (2020) 279–297, https://doi.org/10.1038/s41575-020-0269-9.
[12] R. Vemuri, et al., The microgenderome revealed: sex differences in bidirectional interactions between the microbiota, hormones, immunity and disease susceptibility, Semin. Immunopathol. 41 (2) (2019) 265–275, https://doi.org/10.1007/s00281-018-0716-7.
[13] M. Guo, et al., Gut microbiota and acylcarnitine metabolites connect the beneficial association between estrogen and lipid metabolism disorders in ovariectomized mice, Microbiol. Spectr. (2023) e0014923, https://doi.org/10.1128/spectrum.00149-23.
[14] N. Hasan Alghetaa, et al., Estrobolome dysregulation is associated with altered immunometabolism in a mouse model of endometriosis, Front. Endocrinol. 14 (2023) 1261781, https://doi.org/10.3389/fendo.2023.1261781.
[15] N. Percie du Sert, et al., Reporting animal research: explanation and elaboration for the ARRIVE guidelines 2.0, PLoS Biol. 18 (7) (2020) e3000411, https://doi.org/10.1371/journal.pbio.3000411.
[16] N.R. Council, Guide for the Care and Use of Laboratory Animals, eighth ed., The National Academies Press, Washington, DC, 2011, p. 246.
[17] Strom, J.O., et al., Ovariectomy and 17beta-estradiol replacement in rats and mice: a visual demonstration. J. Vis. Exp. 201264): p. e4013 Doi: 10.3791/4013..
[18] Y. Tian, et al., 17β-oestradiol inhibits ferroptosis in the hippocampus by upregulating DHODH and further improves memory decline after ovariectomy, Redox Biol. 62 (2023) 102708, https://doi.org/10.1016/j.redox.2023.102708.
[19] S. Chen, et al., The combined impact of decabromodiphenyl ether and high fat exposure on non-alcoholic fatty liver disease in vivo and in vitro, Toxicology 464 (2021) 153015, https://doi.org/10.1016/j.tox.2021.153015.
[20] Y.M. Yu, et al., Estrogen deficiency aggravates fluoride-induced liver damage and lipid metabolism disorder in rats, Biol. Trace Elem. Res. 200 (6) (2022) 2767–2776, https://doi.org/10.1007/s12011-021-02857-1.
[21] S. Della Torre, et al., An essential role for liver ERα in coupling hepatic metabolism to the reproductive cycle, Cell Rep. 15 (2) (2016) 360–371, https://doi.org/10.1016/j.celrep.2016.03.019.
[22] A. Pedram, et al., Estrogen reduces lipid content in the liver exclusively from membrane receptor signaling, Sci. Signal. 6 (276) (2013) ra36, https://doi.org/10.1126/scisignal.2004013.
[23] A. Lonardo, et al., Sex differences in nonalcoholic fatty liver disease: state of the art and identification of research gaps, Hepatology 70 (4) (2019) 1457–1469, https://doi.org/10.1002/hep.30626.
[24] J. Kirundi, S. Moghadamrad, C. Urbaniak, Microbiome-liver crosstalk: a multihit therapeutic target for liver disease, World J. Gastroenterol. 29 (11) (2023) 1651–1668, https://doi.org/10.3748/wjg.v29.i11.1651.
[25] W.Q. Yu, et al., CM3-SII polysaccharide obtained from Cordyceps militaris ameliorates hyperlipidemia in heterozygous LDLR-deficient hamsters by modulating gut microbiota and NPC1L1 and PPARα levels, Int. J. Biol. Macromol. 239 (2023) 124293, https://doi.org/10.1016/j.ijbiomac.2023.124293.
[26] S. Gao, et al., Progress of research on the role of active ingredients of Citri Reticulatae Pericarpium in liver injury, Phytomedicine 115 (2023) 154836, https://doi.org/10.1016/j.phymed.2023.154836.
[27] N.H. Sayuti, et al., A review of the effects of fucoxanthin on NAFLD, Nutrients 15 (8) (2023), https://doi.org/10.3390/nu15081954.
[28] C. Yang, et al., Effects of flaxseed powder in improving non-alcoholic fatty liver by regulating gut microbiota-bile acids metabolic pathway through FXR/TGR5 mediating, Biomed. Pharmacother. 163 (2023) 114864, https://doi.org/10.1016/j.biopha.2023.114864.

[29] W.J. Lv, et al., Phytosterols alleviate hyperlipidemia by regulating gut microbiota and cholesterol metabolism in mice, Oxid. Med. Cell. Longev. 2023 (2023) 6409385, https://doi.org/10.1155/2023/6409385.
[30] C. Zhang, et al., Dietary isoquercetin reduces hepatic cholesterol and triglyceride in NAFLD mice by modulating bile acid metabolism via intestinal FXR-FGF15 signaling, J. Agric. Food Chem. 71 (20) (2023) 7723–7733, https://doi.org/10.1021/acs.jafc.3c00952.
[31] J. Vily-Petit, et al., Improvement of energy metabolism associated with NUTRIOSE® soluble fiber, a dietary ingredient exhibiting prebiotic properties, requires intestinal gluconeogenesis, Food Res. Int. 167 (2023) 112723, https://doi.org/10.1016/j.foodres.2023.112723.
[32] J. Mayneris-Perxachs, et al., Gut microbiota steroid sexual dimorphism and its impact on gonadal steroids: influences of obesity and menopausal status, Microbiome 8 (1) (2020) 136, https://doi.org/10.1186/s40168-020-00913-x.
[33] H. Homma, et al., The female intestine is more resistant than the male intestine to gut injury and inflammation when subjected to conditions associated with shock states, Am. J. Physiol. Gastrointest. Liver Physiol. 288 (3) (2005) G466–G472, https://doi.org/10.1152/ajpgi.00036.2004.
[34] K. Kaliannan, et al., Estrogen-mediated gut microbiome alterations influence sexual dimorphism in metabolic syndrome in mice, Microbiome 6 (1) (2018) 205, https://doi.org/10.1186/s40168-018-0587-0.
[35] N.R. Shin, T.W. Whon, J.W. Bae, Proteobacteria: microbial signature of dysbiosis in gut microbiota, Trends Biotechnol. 33 (9) (2015) 496–503, https://doi.org/10.1016/j.tibtech.2015.06.011.
[36] P.H. Bradley, K.S. Pollard, Proteobacteria explain significant functional variability in the human gut microbiome, Microbiome 5 (1) (2017) 36, https://doi.org/10.1186/s40168-017-0244-z.
[37] R. Ganesan, et al., Characteristics of microbiome-derived metabolomics according to the progression of alcoholic liver disease, Hepatol Int (2023), https://doi.org/10.1007/s12072-023-10518-9.
[38] A. Ahmad, et al., Analysis of gut microbiota of obese individuals with type 2 diabetes and healthy individuals, PLoS One 14 (12) (2019) e0226372, https://doi.org/10.1371/journal.pone.0226372.
[39] B. Abdullah, et al., Gut microbiota in pregnant Malaysian women: a comparison between trimesters, body mass index and gestational diabetes status, BMC Pregnancy Childbirth 22 (1) (2022) 152, https://doi.org/10.1186/s12884-022-04472-x.
[40] A. Zhuge, et al., Longitudinal 16S rRNA sequencing reveals relationships among alterations of gut microbiota and nonalcoholic fatty liver disease progression in mice, Microbiol. Spectr. 10 (3) (2022) e0004722, https://doi.org/10.1128/spectrum.00047-22.
[41] T. Ju, et al., The gut commensal Escherichia coli aggravates high-fat-diet-induced obesity and insulin resistance in mice, Appl. Environ. Microbiol. 89 (3) (2023) e0162822, https://doi.org/10.1128/aem.01628-22.
[42] J.A. Santos-Marcos, et al., Influence of gender and menopausal status on gut microbiota, Maturitas 116 (2018) 43–53, https://doi.org/10.1016/j.maturitas.2018.07.008.
[43] Z. Ren, et al., Gut microbiome analysis as a tool towards targeted non-invasive biomarkers for early hepatocellular carcinoma, Gut 68 (6) (2019) 1014–1023, https://doi.org/10.1136/gutjnl-2017-315084.
[44] J. Boursier, et al., The severity of nonalcoholic fatty liver disease is associated with gut dysbiosis and shift in the metabolic function of the gut microbiota, Hepatology 63 (3) (2016) 764–775, https://doi.org/10.1002/hep.28356.
[45] F. Del Chierico, et al., Gut microbiota profiling of pediatric nonalcoholic fatty liver disease and obese patients unveiled by an integrated meta-omics-based approach, Hepatology 65 (2) (2017) 451–464, https://doi.org/10.1002/hep.28572.
[46] X. Qi, et al., The impact of the gut microbiota on the reproductive and metabolic endocrine system, Gut Microb. 13 (1) (2021) 1–21, https://doi.org/10.1080/19490976.2021.1894070.
[47] K.L. Chen, Z. Madak-Erdogan, Estrogen and microbiota crosstalk: should we pay attention? Trends Endocrinol. Metabol. 27 (11) (2016) 752–755, https://doi.org/10.1016/j.tem.2016.08.001.
[48] R. Flores, et al., Fecal microbial determinants of fecal and systemic estrogens and estrogen metabolites: a cross-sectional study, J. Transl. Med. 10 (2012) 253, https://doi.org/10.1186/1479-5876-10-253.
[49] L.M. Leonard, M.S. Choi, T.L. Cross, Maximizing the estrogenic potential of soy isoflavones through the gut microbiome: implication for cardiometabolic health in postmenopausal women, Nutrients 14 (3) (2022), https://doi.org/10.3390/nu14030553.
[50] M.X. Wang, Z.G. Peng, 17β-hydroxysteroid dehydrogenases in the progression of nonalcoholic fatty liver disease, Pharmacol. Ther. (2023) 108428, https://doi.org/10.1016/j.pharmthera.2023.108428.
[51] H.J. Sun, et al., DR region of NKAα1 is a target to ameliorate hepatic lipid metabolism disturbance in obese mice, Metabolism (2023) 155579, https://doi.org/10.1016/j.metabol.2023.155579.
[52] M. Yao, et al., Mitochondrial carnitine palmitoyltransferase-II dysfunction: a possible novel mechanism for nonalcoholic fatty liver disease in hepatocarcinogenesis, World J. Gastroenterol. 29 (12) (2023) 1765–1778, https://doi.org/10.3748/wjg.v29.i12.1765.
[53] A. Poli, C. Agostoni, F. Visioli, Dietary fatty acids and inflammation: focus on the n-6 series, Int. J. Mol. Sci. 24 (5) (2023), https://doi.org/10.3390/ijms24054567.
[54] E. Aaes-Jorgensen, et al., Essential fatty acid deficiency. II. In adult rats, J. Nutr. 66 (2) (1958) 245–259, https://doi.org/10.1093/jn/66.2.245.
[55] S.C. Cunnane, P. Guesnet, Linoleic acid recommendations–A house of cards, Prostaglandins Leukot. Essent. Fatty Acids 85 (6) (2011) 399–402, https://doi.org/10.1016/j.plefa.2011.09.003.
[56] T.N.K. Mäkelä, et al., Associations of serum n-3 and n-6 polyunsaturated fatty acids with prevalence and incidence of nonalcoholic fatty liver disease, Am. J. Clin. Nutr. 116 (3) (2022) 759–770, https://doi.org/10.1093/ajcn/nqac150.
[57] J.E. Kaikkonen, et al., Associations of serum fatty acid proportions with obesity, insulin resistance, blood pressure, and fatty liver: the cardiovascular risk in young Finns study, J. Nutr. 151 (4) (2021) 970–978, https://doi.org/10.1093/jn/nxaa409.
[58] M. Garaulet, et al., Site-specific differences in the fatty acid composition of abdominal adipose tissue in an obese population from a Mediterranean area: relation with dietary fatty acids, plasma lipid profile, serum insulin, and central obesity, Am. J. Clin. Nutr. 74 (5) (2001) 585–591, https://doi.org/10.1093/ajcn/74.5.585.
[59] K. Nimptsch, G. Berg-Beckhoff, J. Linseisen, Effect of dietary fatty acid intake on prospective weight change in the Heidelberg cohort of the European Prospective Investigation into Cancer and Nutrition, Publ. Health Nutr. 13 (10) (2010) 1636–1646, https://doi.org/10.1017/s1368980009993041.
[60] C.E. Ramsden, et al., Use of dietary linoleic acid for secondary prevention of coronary heart disease and death: evaluation of recovered data from the Sydney Diet Heart Study and updated meta-analysis, BMJ 346 (2013) e8707, https://doi.org/10.1136/bmj.e8707.
[61] B. Choque, et al., Dietary linoleic acid requirements in the presence of alpha-linolenic acid are lower than the historical 2 % of energy intake value, study in rats, Br. J. Nutr. 113 (7) (2015) 1056–1068, https://doi.org/10.1017/S0007114515000094.
[62] T.C. Chen, et al., Effect of omega-6 linoleic acid on neurobehavioral development in Caenorhabditis elegans, Prostaglandins Leukot. Essent. Fatty Acids 191 (2023) 102557, https://doi.org/10.1016/j.plefa.2023.102557.
[63] C. Ma, et al., NAFLD causes selective CD4(+) T lymphocyte loss and promotes hepatocarcinogenesis, Nature 531 (7593) (2016) 253–257, https://doi.org/10.1038/nature16969.
[64] J.M. Alessandri, et al., Ovariectomy and 17β-estradiol alter transcription of lipid metabolism genes and proportions of neo-formed n-3 and n-6 long-chain polyunsaturated fatty acids differently in brain and liver, J. Nutr. Biochem. 22 (9) (2011) 820–827, https://doi.org/10.1016/j.jnutbio.2010.07.005.
[65] S.H. Gerges, A.O.S. El-Kadi, Sexual dimorphism in the expression of cytochrome P450 enzymes in rat heart, liver, kidney, lung, brain, and small intestine, Drug Metab. Dispos. 51 (1) (2023) 81–94, https://doi.org/10.1124/dmd.122.000915.
[66] O. Pelkonen, et al., Inhibition and induction of human cytochrome P450 enzymes: current status, Arch. Toxicol. 82 (10) (2008) 667–715, https://doi.org/10.1007/s00204-008-0332-8.
[67] D.J. Waxman, M.G. Holloway, Sex differences in the expression of hepatic drug metabolizing enzymes, Mol. Pharmacol. 76 (2) (2009) 215–228, https://doi.org/10.1124/mol.109.056705.
[68] F. Franconi, et al., Gender differences in drug responses, Pharmacol. Res. 55 (2) (2007) 81–95, https://doi.org/10.1016/j.phrs.2006.11.001.

[69] G.R. Robertson, G.C. Farrell, C. Liddle, Sexually dimorphic expression of rat CYP3A9 and CYP3A18 genes is regulated by growth hormone, Biochem. Biophys. Res. Commun. 242 (1) (1998) 57–60, https://doi.org/10.1006/bbrc.1997.7904.
[70] R. Jamwal, et al., Nonalcoholic fatty liver disease and diabetes are associated with decreased CYP3A4 protein expression and activity in human liver, Mol. Pharm. 15 (7) (2018) 2621–2632, https://doi.org/10.1021/acs.molpharmaceut.8b00159.
[71] S.Y. Choi, et al., Isoform-specific regulation of cytochrome P450 expression and activity by estradiol in female rats, Biochem. Pharmacol. 81 (6) (2011) 777–782, https://doi.org/10.1016/j.bcp.2010.12.019.
[72] Y. Zhu, et al., The alteration of drug metabolism enzymes and pharmacokinetic parameters in nonalcoholic fatty liver disease: current animal models and clinical practice, Drug Metab. Rev. (2023) 1–18, https://doi.org/10.1080/03602532.2023.2202359.
[73] Y. Xu, et al., Hypercholesterolemia reduces the expression and function of hepatic drug metabolizing enzymes and transporters in rats, Toxicol. Lett. 364 (2022) 1–11, https://doi.org/10.1016/j.toxlet.2022.05.009.
[74] L. Zhang, et al., Diet-induced obese alters the expression and function of hepatic drug-metabolizing enzymes and transporters in rats, Biochem. Pharmacol. 164 (2019) 368–376, https://doi.org/10.1016/j.bcp.2019.05.002.
[75] P. Wang, et al., Impact of obese levels on the hepatic expression of nuclear receptors and drug-metabolizing enzymes in adult and offspring mice, Acta Pharm. Sin. B 10 (1) (2020) 171–185, https://doi.org/10.1016/j.apsb.2019.10.009.
[76] S. Hummasti, et al., HRASLS3 is a PPARgamma-selective target gene that promotes adipocyte differentiation, J. Lipid Res. 49 (12) (2008) 2535–2544, https://doi.org/10.1194/jlr.M800269-JLR200.
[77] K. Jaworski, et al., AdPLA ablation increases lipolysis and prevents obesity induced by high-fat feeding or leptin deficiency, Nat. Med. 15 (2) (2009) 159–168, https://doi.org/10.1038/nm.1904.
[78] S.Y. Zhang, et al., Adipocyte-derived lysophosphatidylcholine activates adipocyte and adipose tissue macrophage nod-like receptor protein 3 inflammasomes mediating homocysteine-induced insulin resistance, EBioMedicine 31 (2018) 202–216, https://doi.org/10.1016/j.ebiom.2018.04.022.
[79] C.H. Wang, et al., Phospholipase A/Acyltransferase enzyme activity of H-rev107 inhibits the H-RAS signaling pathway, J. Biomed. Sci. 21 (1) (2014) 36, https://doi.org/10.1186/1423-0127-21-36.
[80] H. Morishita, et al., Organelle degradation in the lens by PLAAT phospholipases, Nature 592 (7855) (2021) 634–638, https://doi.org/10.1038/s41586-021-03439-w.
[81] L. Yang, et al., Targeting PLA2G16, a lipid metabolism gene, by Ginsenoside Compound K to suppress the malignant progression of colorectal cancer, J. Adv. Res. 36 (2022) 265–276, https://doi.org/10.1016/j.jare.2021.06.009.
[82] J. Baggen, et al., Bypassing pan-enterovirus host factor PLA2G16, Nat. Commun. 10 (1) (2019) 3171, https://doi.org/10.1038/s41467-019-11256-z.
[83] T. Uyama, et al., Interaction of phospholipase A/acyltransferase-3 with Pex19p: a possible involvement in the down-regulation of peroxisomes, J. Biol. Chem. 290 (28) (2015) 17520–17534, https://doi.org/10.1074/jbc.M114.635433.